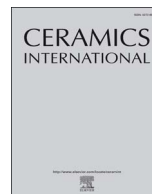




Contents lists available at ScienceDirect

Ceramics International

journal homepage: [www.elsevier.com/locate/ceramint](http://www.elsevier.com/locate/ceramint)

# Formation of CoFe<sub>2</sub>O<sub>4</sub>/PVA-SiO<sub>2</sub> nanocomposites: Effect of diol chain length on the structure and magnetic properties

Thomas Dippong<sup>a</sup>, Oana Cadar<sup>b,\*</sup>, Erika Andrea Levei<sup>b</sup>, Iosif-Grigore Deac<sup>c</sup>, Gheorghe Borodi<sup>d</sup>

<sup>a</sup> Technical University of Cluj-Napoca, North University Center of Baia Mare, Department of Chemistry and Biology, 76 Victoriei Street, 430122 Baia Mare, Romania

<sup>b</sup> INCDO-INOE 2000, Research Institute for Analytical Instrumentation, 67 Donath Street, 400293 Cluj-Napoca, Romania

<sup>c</sup> Babes-Bolyai University, Faculty of Physics, 1 M. Kogalniceanu Street, 400084 Cluj-Napoca, Romania

<sup>d</sup> National Institute for Research and Development of Isotopic and Molecular Technologies, 67-103 Donath Street, 400293 Cluj-Napoca, Romania

## ARTICLE INFO

### Keywords:

Cobalt ferrite  
Diol  
Hybrid matrix  
Co-olivine  
Nanocomposite

## ABSTRACT

The paper presents the influence of diol (1,2-ethanediol, 1,2-propanediol, 1,3-propanediol and 1,4-butanediol) on the formation of magnetic crystalline cobalt ferrite embedded in polyvinyl alcohol-silica hybrid matrix at 200 °C. Formation of crystalline oxides (CoFe<sub>2</sub>O<sub>4</sub>, Co<sub>3</sub>O<sub>4</sub> and Co<sub>2</sub>SiO<sub>4</sub>) was studied by X-ray diffraction and Fourier transformed infrared spectroscopy. The effect of annealing temperature and diol chain length on the cobalt ferrite nanocrystallites size was investigated. Using transmission electron microscopy, the size and shape of particles obtained at 200 °C were recorded and compared to those obtained by annealing at 500, 800 and 1100 °C. The saturation magnetization (M<sub>s</sub>) and coercive field were calculated from the magnetic hysteresis loops of nanocomposites. The M<sub>s</sub> was influenced by the particle size and crystallinity only for nanocomposites annealed at 800 and 1100 °C, when the magnetic domains started to form and to be larger than the critical particle size. The diols used in the synthesis influence both the oxidic phase formation and its properties.

## 1. Introduction

Magnetic nanoparticles have received much attention due to their interesting and significantly different properties from their corresponding bulk materials [1,2]. Ferrimagnetic spinel oxides as cobalt ferrite (CF) exhibit high magnetic anisotropy and coercivity, moderate saturation magnetization (M<sub>s</sub>), remarkable chemical stability and mechanical hardness. These properties recommend them to be used in anti-reflective coatings, optical-chemical sensors, high-density magnetic recording media, magnetic and targeted drug delivery systems, magnetic refrigeration, magnetic stress sensors, transformer cores, recording heads, antenna rods, loading coils, microwave devices, catalysis, solar energy conversion and biomedical sensors [3–15].

Polyvinyl alcohol (PVA) is one of the most used polymers in the matrix assisted synthesis of nanocomposites (NCs) due to its elasticity, resistance to mechanical stress, high hydrophilicity, processability, biocompatibility and good chemical resistance [5]. Silica is another important inert and thermally stable compound used to control the nanoparticles (NPs) agglomeration tendency and their particle size. The cross-linking of silica with PVA produces hybrids with enhanced thermal and chemical stability [3].

The particle size, surface defects/ligands and temperature influence

the intrinsic magnetic properties of CF, while the magnetization within a single domain particle strongly depends on the magnetic anisotropy and the particle's shape [16–18]. The magnetocrystalline anisotropy of CF (380 kJ/m<sup>3</sup>) is much higher than that of Fe<sub>3</sub>O<sub>4</sub> (14 kJ/m<sup>3</sup>) and can be maintained by controlling the magnetic moment of oxides. The magnetic responses are dependent on the Co/Fe ratio and the distribution of Co<sup>2+</sup> and Fe<sup>3+</sup> cations between the tetrahedral and octahedral sites of the spinel [16]. For small particle sizes, the coercivity (H<sub>c</sub>) increases to a maximum and then decreases towards zero [18]. Superparamagnetic NPs become magnetic in the presence of an external magnetic field, but revert to a non-magnetic state when the external field is removed [18]. In the superparamagnetic state, the thermal energy becomes strong enough to demagnetize the saturated magnetic NPs [16].

Our previous studies described the synthesis and characterization of CF embedded in silica matrix using 1,2-ethanediol (1,2ED), 1,2-propanediol (1,2PD), 1,3-propanediol (1,3PD), Fe(III) and Co(II) nitrates and tetraethylortosilicate (TEOS) as reactants, followed by thermal treatment [16,19]. In this study, NCs based on cobalt oxides (CoFe<sub>2</sub>O<sub>4</sub>, Co<sub>3</sub>O<sub>4</sub>, Co<sub>2</sub>SiO<sub>4</sub>) and hybrid PVA-SiO<sub>2</sub> matrix were synthesized at 200, 500, 800 and 1100 °C, using Fe(III) and Co(II) nitrates and diols (1,2ED, 1,2PD, 1,3PD or 1,4-butanediol (1,4BD)). The evolution of the reactions

\* Corresponding author.

E-mail address: [oana.cadar@icia.ro](mailto:oana.cadar@icia.ro) (O. Cadar).

<https://doi.org/10.1016/j.ceramint.2018.03.065>

Received 26 February 2018; Received in revised form 8 March 2018; Accepted 8 March 2018  
0272-8842/ © 2018 Elsevier Ltd and Techna Group S.r.l. All rights reserved.

and crystalline phases were investigated by Fourier transformed infrared spectroscopy (FT-IR) and X-ray diffraction (XRD), while the shape, morphology and size distribution of the NPs were investigated by transmission electron microscopy (TEM). The magnetic properties ( $M_s$ ,  $M_r$ -remanent magnetization and  $H_c$ ) were measured using a vibrating sample magnetometer (VSM).

## 2. Materials and methods

For the synthesis of CF/1,2ED/SP, CF/1,2PD/SP, CF/1,3PD/SP, CF/1,4BD/SP NCs, analytical grade reagents (Merck) were used without further purification. PVA with an average molecular weight of 145,000 g/mol (hydrolysis degree 98%) was used. A 3% PVA solution was prepared by dissolving PVA in deionized water acidulated with 65%  $\text{HNO}_3$ , at 85 °C, under vigorous stirring. **Solution A:**  $\text{Co}(\text{NO}_3)_2 \cdot 6\text{H}_2\text{O}$  and  $\text{Fe}(\text{NO}_3)_3 \cdot 9\text{H}_2\text{O}$  were dissolved in deionized water at room temperature, followed by the addition of diol (1,2ED, 1,2PD, 1,3PD or 1,4BD) in molar ratio of 1:2:8. **Solution B:** 3% PVA solution was added to TEOS- $\text{H}_2\text{O}$ -Ethanol (PVA:TEOS: $\text{H}_2\text{O}$ :Ethanol = 0.03:6.5:10:6.5, molar ratio) under vigorous stirring (reported for 1 mol of  $\text{Co}(\text{NO}_3)_2 \cdot 6\text{H}_2\text{O}$ ). Solutions A and B were mixed together and exposed to air until solidification. The obtained gels were dried at 40 °C for 4 h, heated to 200 °C for 4 h and annealed at 500, 800 and 1100 °C for 5 h.

The XRD patterns were collected on a Shimadzu XRD 6000 diffractometer, using  $\text{Cr K}\alpha$  radiation ( $\lambda = 2.29 \text{ \AA}$ ) in order to remove the fluorescence radiation of Fe, with a graphite monochromator, operated 40 kV and 30 mA, at room temperature. The average nanocrystallites size was estimated using the Scherrer equation (Eq. (1)).

$$D = \frac{0.9\lambda}{\beta \times \cos\theta} \quad (1)$$

where  $\lambda$  is the X-ray wavelength,  $\beta$  is the line broadening at half the maximum intensity (FWHM) after subtracting the instrumental line broadening and  $\theta$  is Bragg angle [20].

The FT-IR spectra were recorded on 1% KBr pellets using a Perkin Elmer Spectrum BX II FT-IR spectrometer. TEM observations carried out on a Hitachi HD2700 electron microscope equipped with digital image recording system and photographic film image, were used to examine the size, shape and clustering of the NPs, while the particle size distributions were determined using the UTHSCSA ImageTool Software. The magnetic measurements were performed with a vibrating sample cryogen-free VSM magnetometer (Cryogenic Limited). The hysteresis loops were recorded in magnetic fields from  $-1$  to  $1$  T at room temperature. Magnetizations vs. magnetic field measurements were performed to find  $M_s$  up to  $5$  T. The samples were embedded in epoxy resin to prevent NPs movement.

## 3. Results and discussion

The formation of crystalline oxides were studied by XRD (Fig. 1). In CF/1,2ED/SP (Fig. 1a), crystalline phases are not identified at 200 and 500 °C. CF (JCPDS card 79-1744) starts to crystallize at 800 °C and appears as highly-crystalline single phase at 1100 °C [21]. In CF/1,2PD/SP (Fig. 1b) and CF/1,3PD/SP (Fig. 1c) at 200 and 500 °C, the presence of  $\text{Co}_3\text{O}_4$  (JCPDS card 80-1536) is observed. At 800 °C, traces of  $\text{CoFe}_2\text{O}_4$  appears beside the well-crystallized  $\text{Co}_3\text{O}_4$ , while at 1100 °C highly crystalline CF is accompanied by Co-olivine traces ( $\text{Co}_2\text{SiO}_4$ , JCPDS card 84-1298) [21]. The formation of  $\text{Co}_3\text{O}_4$  ( $\text{CoO} \cdot \text{Co}_2\text{O}_3$ ) at low temperatures is probably due to the supplementary  $-\text{CH}_2-$  group in the diol, while its disappearance at 1100 °C is the result of the reduction of  $\text{Co}_3\text{O}_4$  to  $\text{CoO}$  at 950 °C [22]. We assume that the formation of crystalline Co-olivine at 1100 °C is a consequence of the reaction between  $\text{CoO}$  and free  $\text{SiO}_2$  that did not react with PVA during matrix formation. In CF/1,4BD/SP (Fig. 1d), low crystalline CF appears at 200 °C, its crystallization increases with the annealing temperature, at 1100 °C highly crystalline single phase CF being observed. The growth

of nanocrystallites' sizes with annealing temperature and diol chain length is presented in Table 1.

Fig. 2 shows the relationship between crystallinity and annealing temperature. The degree of crystallinity was calculated as the ratio of diffraction peaks area and total diffraction area comprising diffraction peaks and amorphous halo. Samples containing only crystalline phases have sharp diffraction peaks of high intensity, whereas samples containing only amorphous phases have broad peaks (amorphous halo). In samples with both crystalline and amorphous phases, the diffraction peaks corresponding to crystalline phase overlaps the diffraction halo corresponding to amorphous phase. For our NCs, up to 500 °C, the degree of crystallinity is almost constant, while between 500 and 1100 °C an almost linear increase is observed.

The FT-IR spectra (Fig. 3) of NCs shows a broad band at  $1039\text{--}1073 \text{ cm}^{-1}$  attributed to overlapping of  $\text{Si-O-Si}$  and  $\text{C-C-O}$  stretchings in the hybrid matrix [3,5,23]. The band at  $796\text{--}801 \text{ cm}^{-1}$  is attributed to the symmetric stretching vibration of  $\text{Si-O}$  bond in the hybrid PVA- $\text{SiO}_2$  matrix [7,23]. In the spectra of NCs heated at 200, 500 and 800 °C, the shoulder band in the range of  $1130\text{--}1170 \text{ cm}^{-1}$  is attributed to  $\text{Si-O-C}$  bonds formation in the matrix by silica and PVA crosslinking [3]. Except for NCs heated at 200 °C, the formation of CF is confirmed by the broad band at  $556\text{--}593 \text{ cm}^{-1}$  attributed to  $\text{Fe-O}$  stretching vibration in tetrahedral sites and the bands at  $365\text{--}377 \text{ cm}^{-1}$  and  $429\text{--}463 \text{ cm}^{-1}$  attributed to  $\text{Co-O}$  stretching/bending vibrations in octahedral sites [7,8,11]. The difference in band position could be explained by the different length of metal-oxygen bonds in octahedral and tetrahedral sites [23]. The band at  $650\text{--}655 \text{ cm}^{-1}$  in the spectra of CF/1,2PD/SP and CF/1,3PD/SP at 200, 500 and 800 °C is attributed to  $\text{Co-O}$  vibration [11]. The  $854\text{--}857 \text{ cm}^{-1}$  band present only in spectra of CF/1,2PD/SP and CF/1,3PD/SP at 1100 °C is attributed to stretching vibrations of  $\text{SiO}_4$  tetrahedra in Co-olivine ( $\text{Co}_2\text{SiO}_4$ ) [24]. The FT-IR data confirms the formation of PVA- $\text{SiO}_2$  hybrid matrix, CF single phase in CF/1,2ED/SP and CF/1,4BD/SP and  $\text{Co}_3\text{O}_4$  (200, 500, 800 °C) and  $\text{Co}_2\text{SiO}_4$  (1100 °C) beside CF in CF/1,2PD/SP and CF/1,3PD/SP.

TEM images (Fig. 4) reveal non-agglomerated, spherical shape NPs. The growth of NPs with the increase of annealing temperature and diol chain length is also remarked. The particle size distribution calculated from TEM images by analyzing over 100 NPs for each sample, shows particles with size of 9–15 nm at 800 °C and 18–30 nm at 1100 °C, respectively. The average size of CF NPs in CF/1,2ED/SP is 9 nm at 800 °C and 18 nm at 1100 °C, respectively. For CF/1,2PD/SP and CF/1,3PD/SP, the average size of NPs (identified as  $\text{CoFe}_2\text{O}_4$  and  $\text{Co}_3\text{O}_4$  by XRD) is 11 and 13 nm at 800 °C, while at 1100 °C the average size of NPs (identified as  $\text{CoFe}_2\text{O}_4$  and  $\text{Co}_2\text{SiO}_4$  by XRD) is 23 and 25 nm. For CF/1,4BD/SP, the average size of CF NPs is 15 nm (800 °C) and 30 nm (1100 °C), respectively. The low variations of particles size are explained by the weak crystallization of  $\text{CoFe}_2\text{O}_4$  at 800 °C and the strong surface effect that easily gathers the low size crystallites into larger aggregates at 1100 °C [25–27].

The crystallites sizes estimated by XRD data are comparable with the particle sizes obtained by TEM and increase with increasing of annealing temperature and diol chain length. For NCs obtained from 1,2PD and 1,3PD, the nanocrystallite sizes estimated by XRD data are individually calculated for CF and  $\text{Co}_3\text{O}_4$  (800 °C)/CF and  $\text{Co}_2\text{SiO}_4$  (1100 °C), while for TEM, the particle sizes are calculated for all phases. The increase of particles sizes can be attributed to the growth rate of crystals following the volume expansion and supersaturation reduction of the system at high annealing temperatures [24–27]. The NPs sizes increase with temperature as a result of the formation of crystalline clusters which become jointly cemented [25]. TEM confirms the influence of diol chain length on the particle size in case of CF, CF/ $\text{Co}_3\text{O}_4$  and CF/ $\text{Co}_2\text{SiO}_4$  phases.

Figs. 5 and 6 show the magnetic hysteresis loops, magnetization first derivatives ( $\text{dM}/\text{d}(\mu_0\text{H})$ ),  $M_s$  and  $H_c$  values for NCs annealed at 800 and 1000 °C. Based on hysteresis loops and  $M(H)$  curves,  $M_s$ ,  $M_r$  and  $H_c$  values were determined. Generally,  $M_s$  increases with the diol chain

Download English Version:

<https://daneshyari.com/en/article/7887194>

Download Persian Version:

<https://daneshyari.com/article/7887194>

[Daneshyari.com](https://daneshyari.com)